

Supplementary Material

Modulation of splicing catalysis for therapeutic targeting of leukemias with spliceosomal mutations

Stanley Chun-Wei Lee^{1,9}, Heidi Dvinge^{2,3,9}, Eunhee Kim¹, Hana Cho¹, Jean-Baptiste Micol¹, Young Rock Chung¹, Benjamin H. Durham¹, Akihide Yoshimi¹, Young Joon Kim¹, Michael Thomas⁴, Camille Lobry⁵, Chun-Wei Chen⁶, Alessandro Pastore¹, Justin Taylor¹, Xujun Wang⁶, Andrei Krivtsov⁶, Scott A. Armstrong^{6,7}, James Palacino⁴, Silvia Buonamici⁴, Peter G. Smith⁴, Robert K. Bradley^{2,3,10,*}, Omar Abdel-Wahab^{1,8,10,*}

¹Human Oncology and Pathogenesis Program, Memorial Sloan Kettering Cancer Center, New York, NY, USA

²Computational Biology Program, Public Health Sciences Division, Fred Hutchinson Cancer Research Center, Seattle, WA, USA

³Basic Sciences Division, Fred Hutchinson Cancer Research Center, Seattle, WA, USA

⁴H3 Biomedicine, Inc., Cambridge, MA, USA

⁵Institut National de la Santé et de la Recherche Médicale (INSERM) U1170, Institut Gustave Roussy, Villejuif, France

⁶Cancer Biology and Genetics Program, Memorial Sloan Kettering Cancer Center, New York, NY, USA.

⁷Department of Pediatrics, Memorial Sloan Kettering Cancer Center, New York, NY, USA.

⁸Leukemia Service, Dept. of Medicine, Memorial Sloan Kettering Cancer Center, New York, NY, USA

⁹Equal contribution, co-first authors

¹⁰Co-senior authors

*Corresponding Authors:

Robert K. Bradley
Email: rbradley@fredhutch.org

Omar Abdel-Wahab
Email: abdelwao@mskcc.org

Supplementary Figure 1. Generation and characterization of *Srsf2* hemizygous mutant mice. (a) *Srsf2*^{P95H} hemizygous mutant mice and littermate controls were generated by crossing *Mx1-Cre*⁺*Srsf2*^{+/fl} mice to *Srsf2*^{P95H/+} mice. This generated *Mx1-Cre*⁺*Srsf2*^{+/+} control mice, *Mx1-Cre*⁺*Srsf2*^{+/fl} mice (heterozygous knockout; *Mx1-Cre*⁺*Srsf2*^{+/-}), heterozygous mutant (*Mx1-Cre*⁺*Srsf2*^{P95H/+}) mice, and hemizygous mutant (*Mx1-Cre*⁺*Srsf2*^{P95H/-}) mice. (b) Percentage of CD45.2⁺ chimerism in the peripheral blood of CD45.1 recipient mice (*n* = 10 mice/genotype) following plpC administration in competitive BM transplantation. (c) Flow cytometric enumeration of CD45.2⁺ long-term hematopoietic stem (lineage-negative Sca1-c-Kit⁺ (LSK) CD150⁺ CD48⁻) cells in the BM of recipient mice 18-weeks following transplantation with control (*Srsf2*^{+/+}), heterozygous knockout (*Srsf2*^{+/-}), heterozygous mutant (*Srsf2*^{P95H/+}), and hemizygous mutant (*Srsf2*^{P95H/-}) BM cells. (d) Wright-Giemsa staining of peripheral blood smears from non-competitively transplanted mice (scale bars, 5 μm) revealing hypolobated neutrophils in peripheral blood of *Srsf2*^{P95H/+} and *Srsf2*^{P95H/-} mice. (e) Hemoglobin and (f) peripheral blood platelet count of each genotype of mice over 18-weeks of noncompetitive transplantation. (g) Gene Ontology analysis of differentially expressed genes in purified HSPCs from *Srsf2*^{+/-}, *Srsf2*^{P95H/+} and *Srsf2*^{P95H/-} mice relative to *Srsf2*^{+/+} control mice. Error bars represent mean ± SD. **P* < 0.05; ****P* < 0.001; *****P* < 0.0001.

Supplementary Figure 2. The wildtype *Srsf2* allele is required for leukemogenesis in the context of *Srsf2*^{P95H} mutation. (a) Experimental schema used to generate *MLL-AF9* murine leukemia model on the *Srsf2*^{P95H/-} background. *MLL-AF9* cDNA (in an MSCV-IRES-GFP vector) was retrovirally overexpressed in c-Kit-enriched E12.5-14.5 fetal liver cells from *Srsf2*^{P95H/fl} or *Mx1-Cre*⁺*Srsf2*^{P95H/-} mice, and transplanted into lethally irradiated CD45.1 recipient mice via tail-vein injection. Analysis of peripheral blood (PB) (b) white blood cell, (c) red blood cell, and (d) platelet counts over 6 weeks post-polyI:C administration. (e) Analysis of PB GFP percentage and (f) donor-derived (CD45.2 percentage) contribution over 6 weeks post-polyI:C administration. (g) White blood cell count and GFP percentage of *Srsf2*^{P95H/fl} (control) and *Srsf2*^{P95H/-} (hemizygous) mice at week 3 post-plpC administration. The animal indicated by the red square eventually developed AML. (h) Kaplan-Meier survival curves of primary *MLL-AF9/Srsf2*^{P95H/fl} (control) and *MLL-AF9/Srsf2*^{P95H/-} (hemizygous) mice (Mantel-Cox log-ranked test). (i) Genotyping PCR of the *Srsf2* flox allele. DNA samples were extracted from the PB of mice in the pre-leukemic phase (3 wk), and from BM cells at the time of leukemic onset (Sac). Mouse #4 is derived from the same animal boxed in red in (g). (j) Experimental schema to examine the effect of E7107 treatment on the *Srsf2*-wildtype (*Mx1-Cre*⁺*Srsf2*^{+/+}) and *Srsf2*-mutant (*Mx1-Cre*⁺*Srsf2*^{P95H/+}) BM LK (CD45.2⁺ lineage-negative Sca1⁻ cKit⁺) population. Error bars represent mean ± SE. **P* < 0.05; ***P* < 0.01; ****P* < 0.001; *****P* < 0.0001.

Supplementary Figure 3. Generation of *MLL*-rearranged *Srsf2*-wildtype or mutant murine leukemias and sensitivity to E7107. (a) Schematic of protocol used to generate *MLL-AF9* overexpressing leukemias on *Srsf2* wildtype (*Srsf2*^{+/+}) or mutant (*Srsf2*^{P95H/+}) backgrounds. *MLL-AF9* cDNA (in an MSCV-IRES-GFP vector) was retrovirally overexpressed in bone marrow (BM) mononuclear cells harvested from 5-fluorouracil (5-FU)-treated *Vav-Cre*⁺*Srsf2*^{+/+} or *Vav-Cre*⁺*Srsf2*^{P95H/+} mice. Lethally irradiated CD45.1 recipient mice were reconstituted with *MLL-AF9;Srsf2*^{+/+} or *MLL-AF9;Srsf2*^{P95H/+} BM cells by tail-vein injection. (b) Kaplan-Meier survival curves of primary transplant recipient mice (Mantel-Cox log-ranked test). (c) Liver and spleen weight from *MLL-AF9;Srsf2*^{+/+} and *MLL-AF9;Srsf2*^{P95H/+} mice at the time of sacrifice. (d) Gene Ontology analysis of differentially expressed genes in purified leukemic cells (Mac1⁺ GFP⁺) from *MLL-AF9;Srsf2*^{+/+} and *MLL-AF9;Srsf2*^{P95H/+} mice. (e) Flow cytometric characterization of BM, spleen, and peripheral blood of primary recipients from *MLL-AF9;Srsf2*^{+/+} or *MLL-AF9;Srsf2*^{P95H/+} murine leukemias. (f) H&E staining of BM, spleen (scale bars, 100 μm) and liver (scale bars, 200 μm), and (g) BM cytospin (scale bars, 50 μm) from primary *MLL-AF9;Srsf2*^{+/+} and *MLL-AF9;Srsf2*^{P95H/+} mice at the time of sacrifice. (h) H&E staining of BM (scale bars, 100 μm) and liver (scale bars, 200 μm) from recipient mice following 10 days of E7107 treatment.

Peripheral blood hemoglobin (i), and platelet (j) counts following 10 days of E7107 or vehicle treatment in secondary transplant mice. Error bars represent mean \pm SD. * $P < 0.05$; ** $P < 0.01$; *** $P < 0.001$.

Supplementary Figure 4. Global splicing and coding gene expression changes in myeloid leukemias treated with E7107 in *SRSF2*-wildtype or mutant background. (a) Summary of the numbers of up-/down-regulated splicing events and coding genes identified when comparing E7107-treated to untreated samples. (b) Heat map based on most variable cassette exons or retained introns or (c) coding genes in *MLL-AF9*;*Srsf2*^{+/+} or *MLL-AF9*;*Srsf2*^{P95H/+} leukemias following E7107 or vehicle treatment *in vivo*. The majority of the observed variation is genotype-specific. Sample colors as in Fig. 3. Gene expression was normalized with the TMM method¹, and all values were z-score standardized. (d) Cumulative distribution function (CDF) analyses comparing cassette exon splicing (top) and intron retention (bottom) in *MLL-AF9*;*Srsf2*^{+/+} or *MLL-AF9*;*Srsf2*^{P95H/+} leukemias following E7107 or vehicle treatment *in vivo*, using median Ψ values across replicates. Only cassette exons and introns within mouse homologs of genes containing differentially spliced events in at least one of the human *SRSF2*-mutant, *MLL*-rearranged AML samples from Fig. 2c are included. Insert in each plot is zoomed-in to display the difference between the two genotypes. (e) Gene Ontology analysis of differentially expressed genes in purified leukemic cells (Mac1⁺ GFP⁺) from *MLL-AF9*;*Srsf2*^{+/+} and *MLL-AF9*;*Srsf2*^{P95H/+} mice. (f) Western blot analysis of Meis1 and histone H3 lysine 79 dimethylation (H3K79me2) levels in *MLL-AF9*;*Srsf2*^{+/+} and *MLL-AF9*;*Srsf2*^{P95H/+} leukemic cells following 3 days of E7107 treatment (0.5 nM) *in vitro*. Cells were also separately treated with a DOT1L inhibitor, EPZ-4777 (EPZ; 10 μ M), as a positive control for H3K79me2 level following DOT1L inhibition. Actin and histone H3 were used as loading controls. (g) Relative protein levels were quantified by densitometry relative to DMSO-treated cells. Error bars represent mean \pm SD. *** $P < 0.001$; **** $P < 0.0001$.

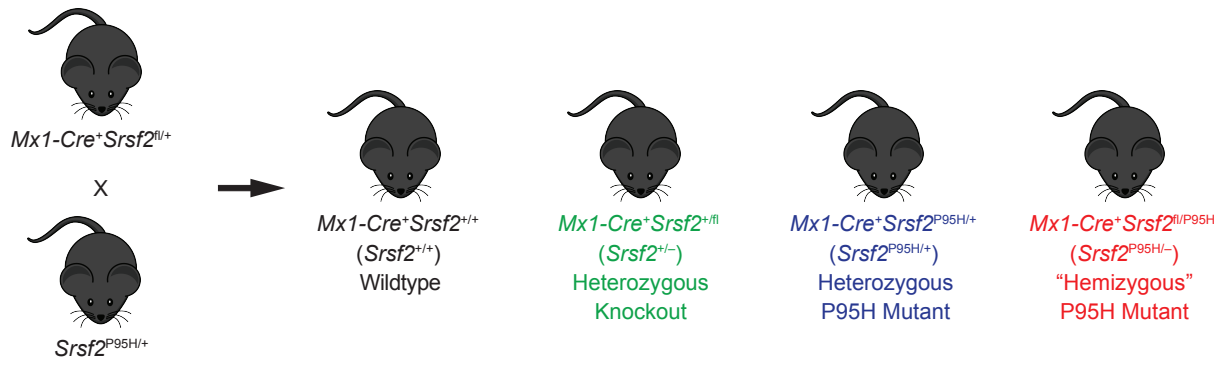
Supplementary Figure 5. Effects of Dot1l and Meis1 restoration on E7107-mediated growth inhibition and rescue of E7107-mediated effects via the SF3B1 R1074H mutation. (a) Confirmation of *DOT1L* cDNA overexpression by western blot of H3K79me2 in *MLL-AF9*;*Srsf2*^{+/+} and *MLL-AF9*;*Srsf2*^{P95H/+} leukemia cells *in vitro*. Histone H3 was used as a loading control. (b) Relative proliferation of *MLL-AF9*;*Srsf2*^{+/+} ($n = 3$ independent biological clones) and *MLL-AF9*;*Srsf2*^{P95H/+} ($n = 4$ independent biological clones) leukemia cells overexpressing *DOT1L* 6 days post E7107 (0.5 nM) or DMSO exposure. (c) Confirmation of *Meis1* cDNA overexpression by qRT-PCR. (d) Relative proliferation of *MLL-AF9*;*Srsf2*^{+/+} ($n = 3$ independent biological clones) and *MLL-AF9*;*Srsf2*^{P95H/+} ($n = 4$ independent biological clones) leukemia cells overexpressing *Meis1* 6 days post E7107 (0.5 nM) or DMSO exposure. (e) Experimental schema to generate stable cell lines expressing N-terminal FLAG tagged *SF3B1* wildtype (WT) or *SF3B1*R1074H using the PiggyBac Transposon system. Confirmation of *SF3B1*WT or *SF3B1*R1074H plasmid integration into *MLL-AF9* leukemia cells by (f) Sanger sequencing (using PCR primers specific for the codon-optimized *SF3B1* wildtype or R1074H cDNA), and (g) validation of protein expression by Western blotting. (h) *In vitro* cell viability assay following 48 hours of E7107 treatment in *MLL-AF9*;*Srsf2*^{P95H/+} parental, (white circle), *MLL-AF9*;*Srsf2*^{P95H/+} *SF3B1*WT- (blue diamond) and *MLL-AF9*;*Srsf2*^{P95H/+} *SF3B1*R1074H- (red square) expressing cells. The numbers in the parentheses correspond to the IC50 value of each cell line 48 hours after E7107 exposure. (i) Qualitative RT-PCR (left) and qRT-PCR (right) analyses quantifying the relative levels of exclusion (EX) and inclusion (IN) isoforms of *Dot1l* and *Meis1* in *MLL-AF9*;*Srsf2*^{P95H/+} parental, *MLL-AF9*;*Srsf2*^{P95H/+};*SF3B1* WT- and *MLL-AF9*;*Srsf2*^{P95H/+};*SF3B1*R1074H-expressing cells, 3 and 6 hours after E7107 (10 nM) or DMSO exposure *in vitro*. Error bars represent mean \pm SD. * $P < 0.05$; ** $P < 0.01$; *** $P < 0.001$; **** $P < 0.0001$.

Supplementary Figure 6. Efficacy of pharmacologic inhibition of splicing in human myeloid leukemias and primary normal human cells. (a) Variant allele frequencies (VAF) of somatic mutations in primary human AML peripheral blood mononuclear cells (PB MNCs) (x-axis) and hCD45⁺ cells purified from 3 vehicle-treated mice engrafted from each patient (y-axis). (b) VAF of mutations from hCD45⁺ cells purified from E7107- (y-axis) versus vehicle-treated (x-axis) mice ($n = 3$ mice per

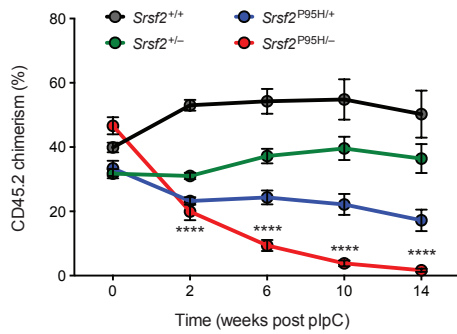
treatment group). Percentage of (c) human stem (hCD45⁺ hCD34⁺ hCD38⁻) and progenitor (hCD45⁺ hCD34⁺ hCD38⁺), (d) lymphoid (hCD45⁺ hCD3⁺ hCD19⁺) and (e) myeloid (hCD45⁺ hCD33⁺) fractions in bone marrow (BM) of NSG mice following 10 days of vehicle or E7107 treatment based on spliceosome mutational status. (f) Experimental schema used to examine the effect of E7107 treatment on apoptosis and cell cycle *in vivo* using primary human AML patient-derived xenograft (PDX) models. Following stable engraftment of human leukemia cells, mice were treated with E7107 (4 mg/kg/day) or vehicle for 5 consecutive days. BrdU was injected 24 hours prior to the last treatment, and mice were sacrificed 3 hours after the fifth E7107 treatment. Apoptosis and cell cycle status of human leukemia cells (hCD45⁺) were determined by Annexin V/PI staining and BrdU incorporation, respectively. Error bars represent mean \pm SD. * $P < 0.05$; ** $P < 0.01$; *** $P < 0.001$.

Supplementary Figure 1

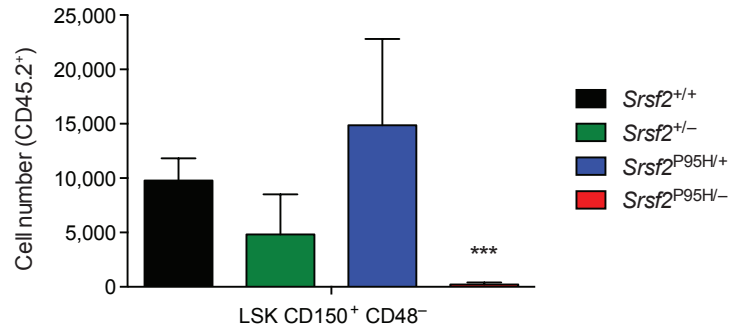
a



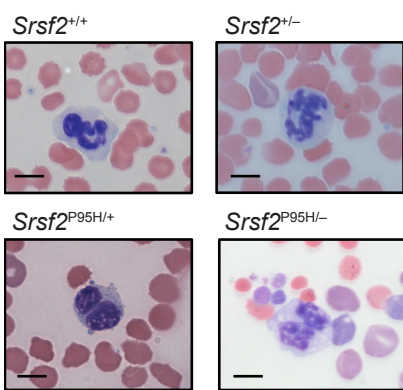
b



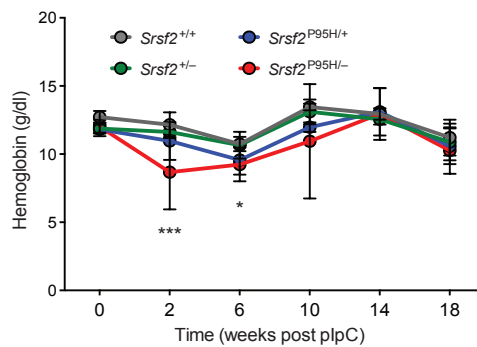
c



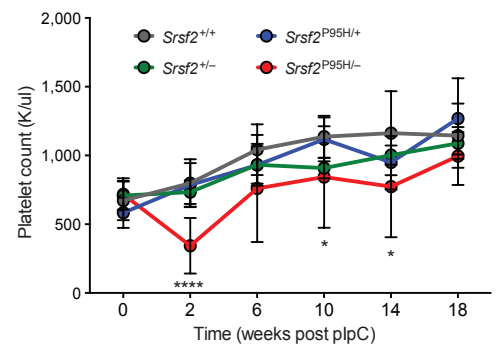
d



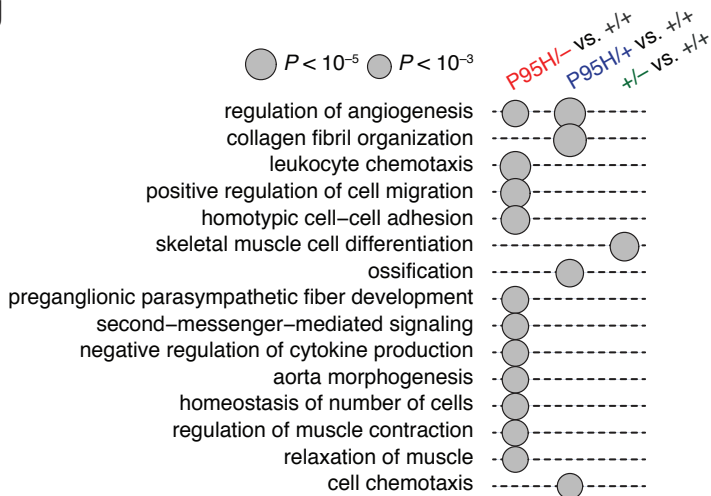
e



f

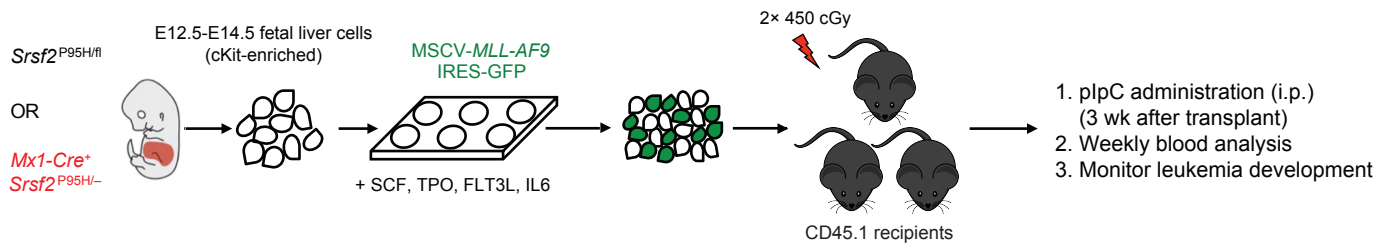


g

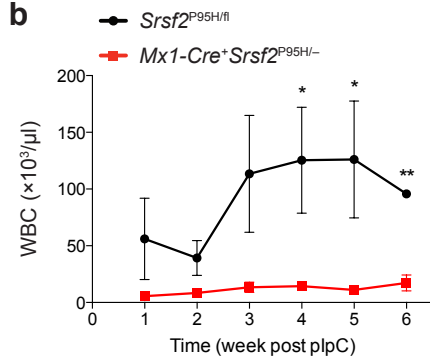


Supplementary Figure 2

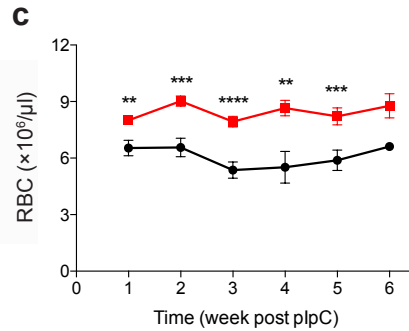
a



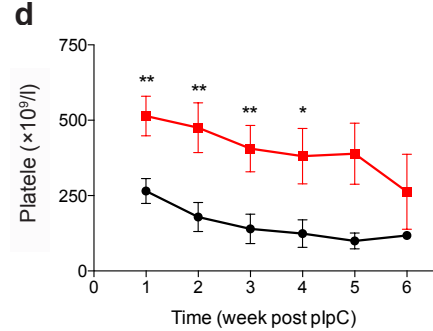
b



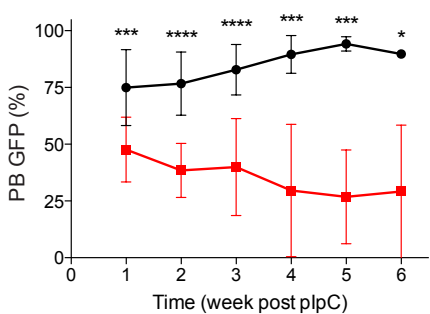
c



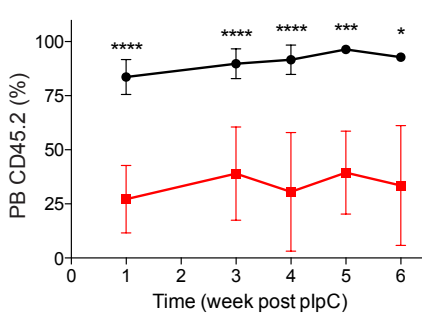
d



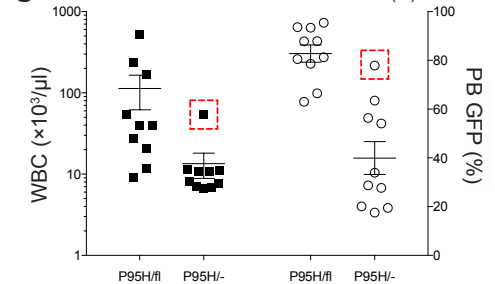
e



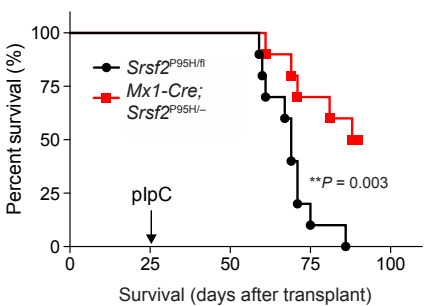
f



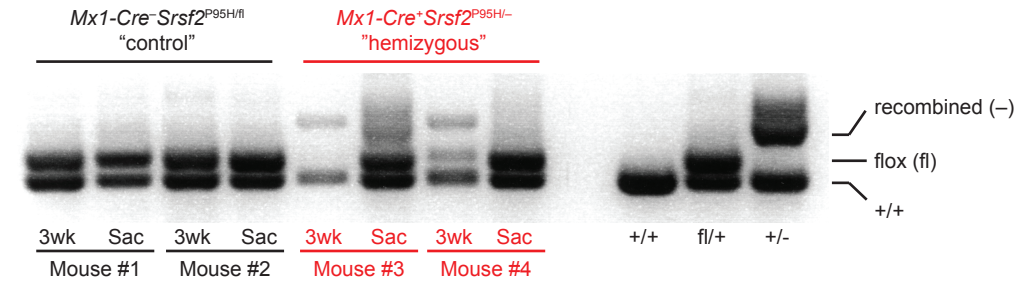
g



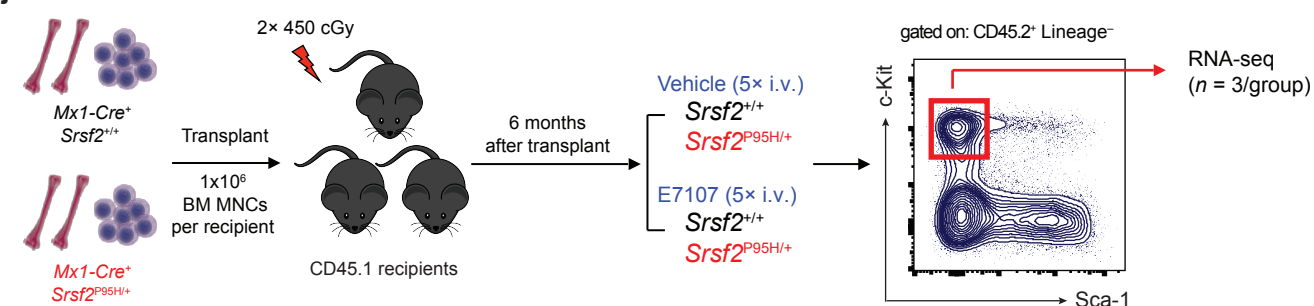
h



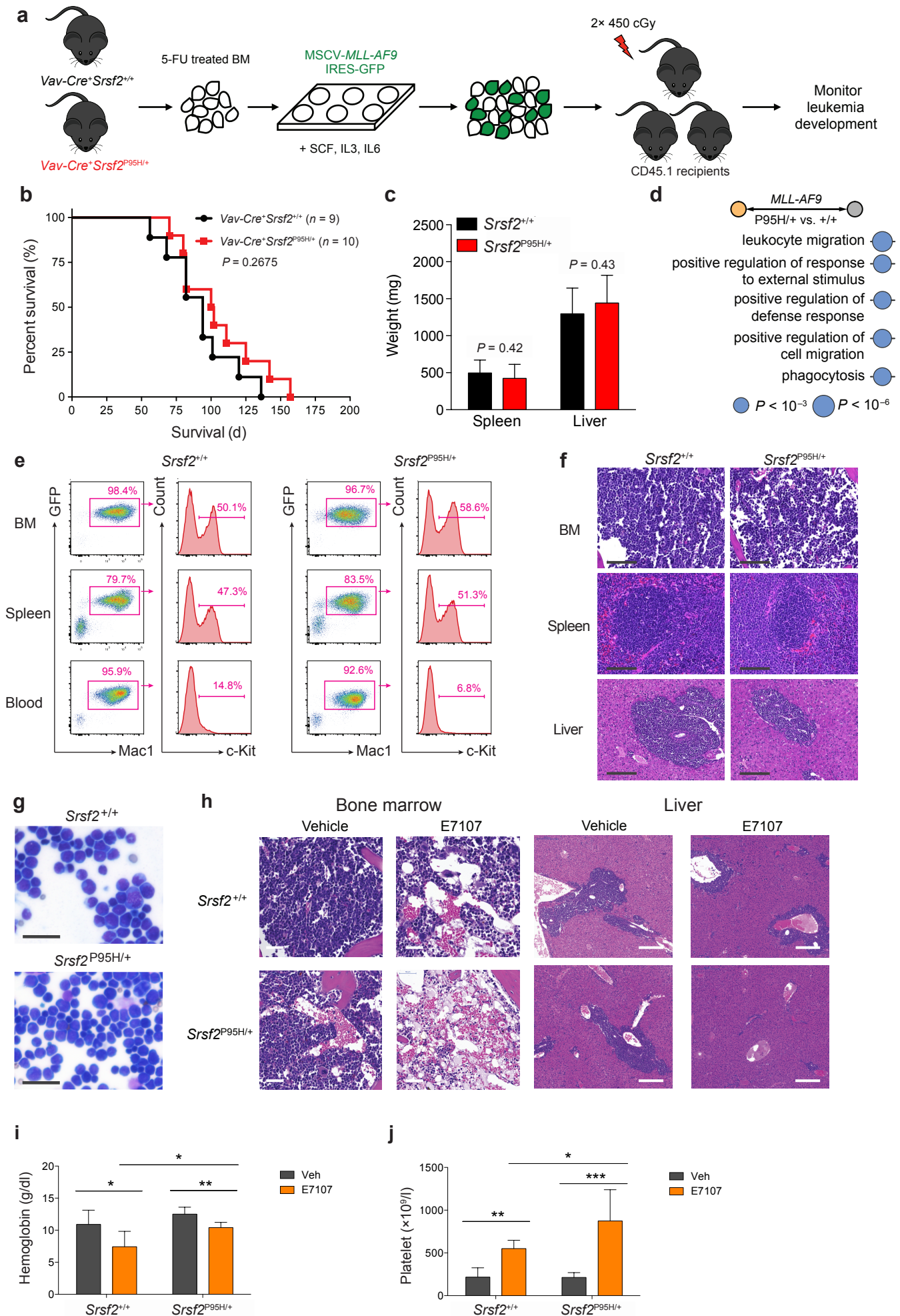
i



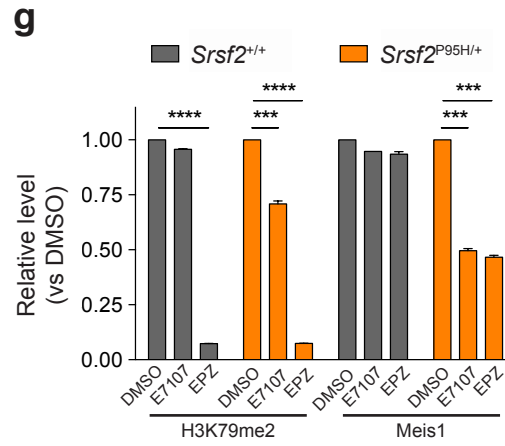
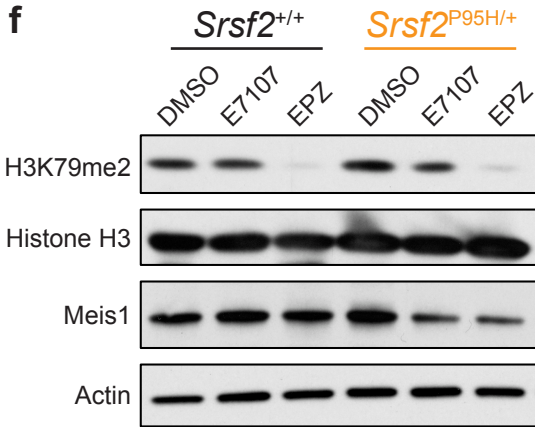
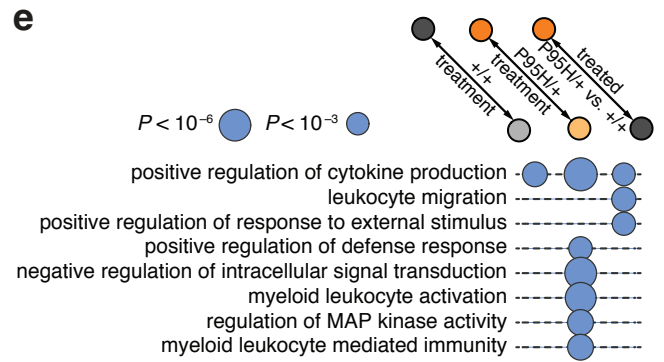
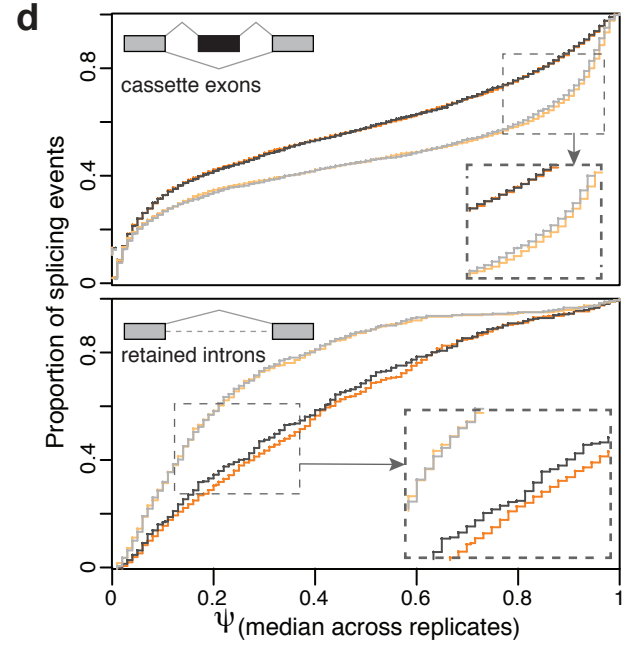
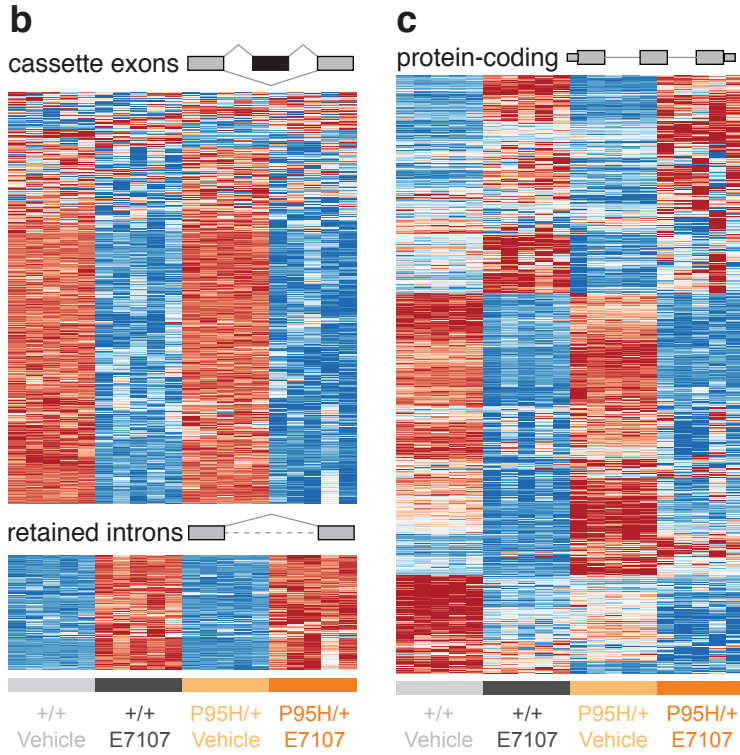
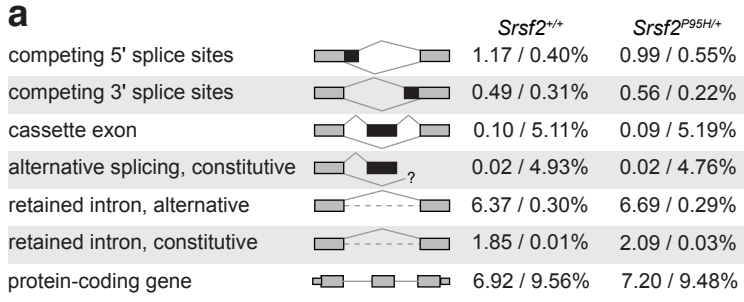
j



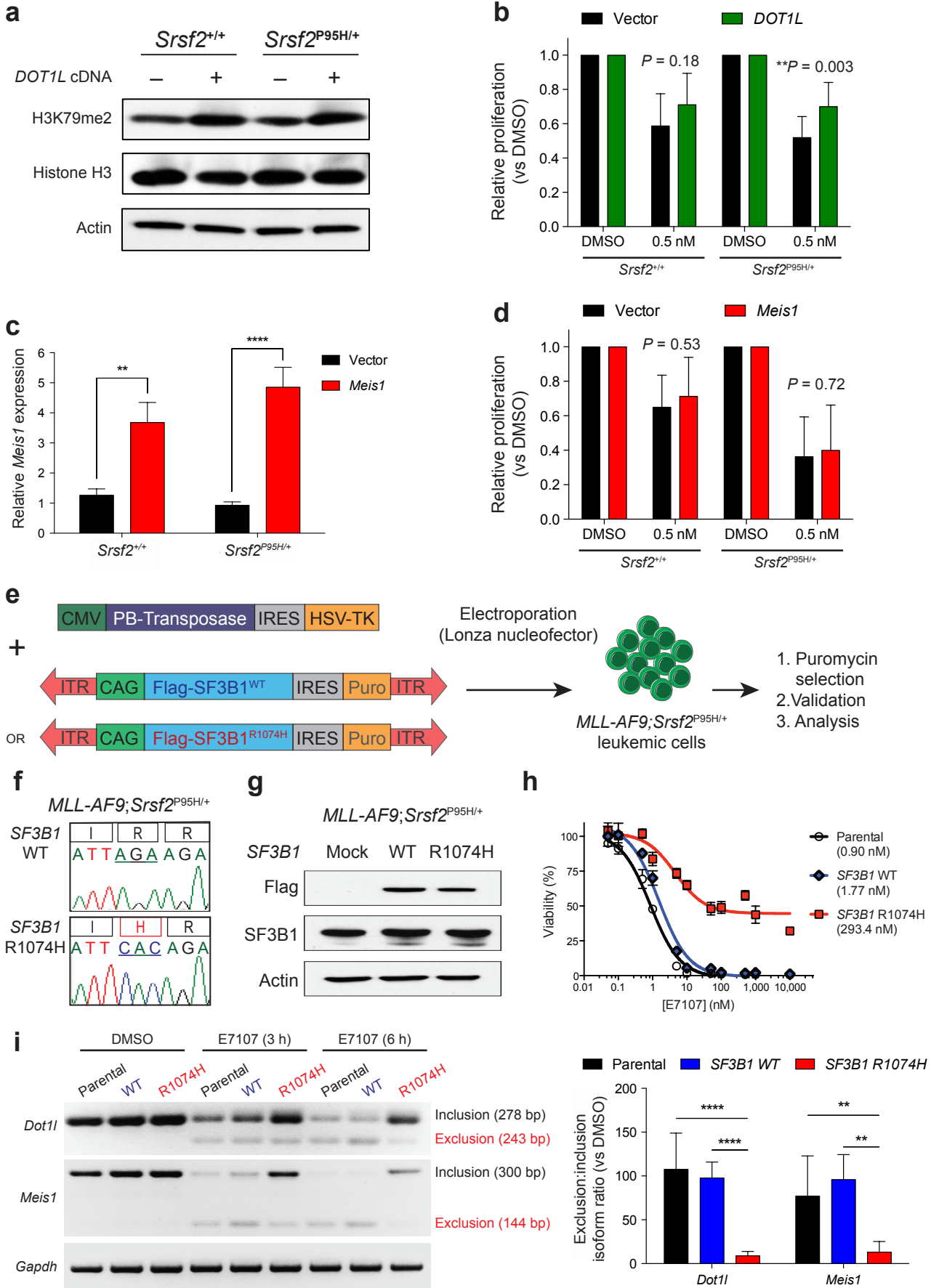
Supplementary Figure 3



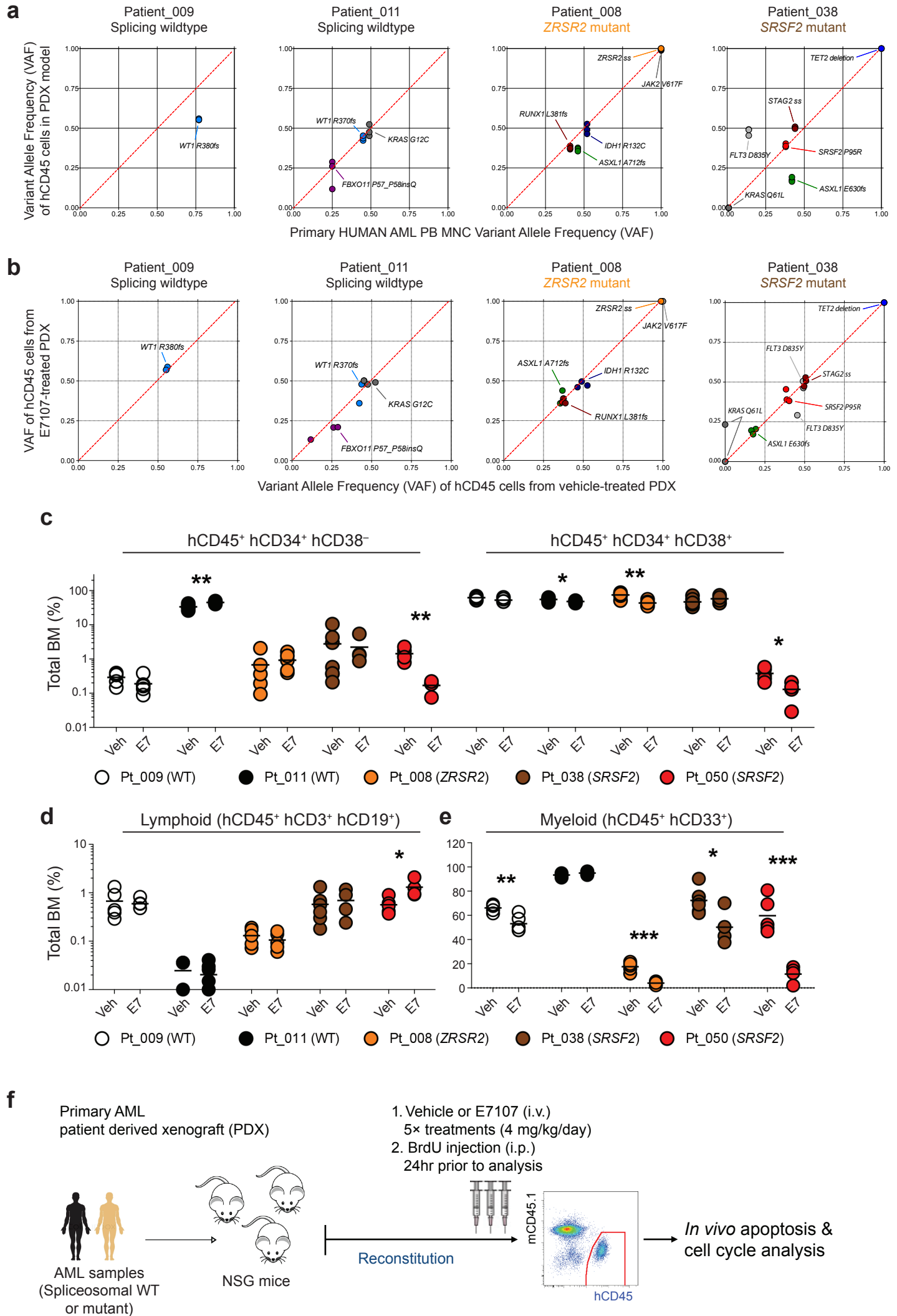
Supplementary Figure 4



Supplementary Figure 5



Supplementary Figure 6



Supplementary Table 1: Median normalized gene expression values across replicates in each of the murine mRNA sequencing experiments shown in Figures 1-3. Gene expression values averaged across replicates within each dataset are provided.

Supplementary Table 2: Frequency of differential splicing for different classes of splicing events associated with *Srsf2* alterations. From top to bottom, numbers indicate the percentage of increases/decreases in usage of intron-proximal 5' splice sites, usage of intron-proximal 3' splice sites, inclusion of cassette exons, canonical splicing of annotated constitutive splice junctions, removal of introns annotated as alternative, and removal of introns annotated as constitutive. Frequency is relative to the total number of splicing events that could be detected within each comparison.

		<u>+/- vs. +/+</u>	<u>P95H/+ vs. +/+</u>	<u>P95H/- vs. +/+</u>
competing 5' splice sites		0.36 / 0.53%	0.77 / 0.70%	0.99 / 1.91%
competing 3' splice sites		0.21 / 0.38%	0.35 / 0.47%	0.61 / 0.84%
cassette exon		0.44 / 0.53%	1.17 / 1.67%	1.86 / 3.03%
alternative splicing, constitutive		0.09 / 0.10%	0.16 / 0.32%	0.29 / 0.55%
retained intron, alternative		0.50 / 0.18%	0.55 / 0.19%	5.04 / 0.56%
retained intron, constitutive		0.32 / 0.09%	0.18 / 0.12%	0.63 / 0.21%

Supplementary Table 3: Median exon inclusion rates (PSI (percent spliced in) values (ψ)) for cassette exons across replicates in each of the murine mRNA sequencing experiments shown in Figures 1-3. PSI values averaged across replicates within each dataset are shown.

Supplementary Table 4: Genetic characteristics of primary AML patients used in patient-derived xenograft (PDX) models. Spliceosomal gene mutations are shown in red font.

Patient ID	Diagnosis & Blast percentage	Cytogenetics	Somatic Mutations
Pt_009	Relapsed AML Blast = 40.1%	Add (1p) Del5q Del11q Del12p Inv chromosome 5	WT1_R380fs*72
Pt_011	Relapsed AML Blast = 40%	MLL-ENL	FBXO11_P49_Q50insQ KRAS_G12C WT1_R370fs*15
Pt_026	Relapsed AML Blast = 57%	Trisomy 4 Inv chromosome 3	NPM1_W288fs*10 TET2_Q690*
Pt_008	Relapsed AML Blast = 60%	Del1p Trisomy 13 MLL-EP300	ASXL1_M723fs*3 IDH1_R132C JAK2_V617F RUNX1_P383fs*101 ZRSR2_splice_399+1G>C
Pt_038	De novo AML Blast = 33.6%	Trisomy 13	ASXL1_E635fs*15 FLT3_D835Y KRAS_G12D KRAS_Q61L SRSF2_P95_P96insR STAG2_splice_894-2A>G TET2 deletion
Pt_050	Relapsed AML Blast = 55%	Del7q	CEBPA_R165fs*6 NPM1_W288fs*10 SRSF2_P95L TET2_Q417* TET2_S1286F TP53_R175H

References:

1. Robinson, M.D. & Oshlack, A. A scaling normalization method for differential expression analysis of RNA-seq data. *Genome biology* **11**, R25 (2010).